

The Numerical Solution of Nekrasov's Equation in the Boundary Layer near the Crest, for Waves near the Maximum Height

by J.G. Byatt-Smith

Department of Mathematics and Statistics
University of Edinburgh.

Key Words: Integral equations, water waves.

Abstract: Nekrasov's integral equation describing water waves of permanent form, determines the angle $\phi(s)$ that the wave surface makes with the horizontal. The independent variable s is a suitably scaled velocity potential, evaluated at the free surface, with the origin corresponding to the crest of the wave. For all waves, except for amplitudes near the maximum, $\phi(s)$ satisfies the inequality $|\phi(s)| < \pi/6$.

It has been shown numerically and analytically, that as the wave amplitude approaches its maximum, the maximum of $|\phi(s)|$ can exceed $\pi/6$ by about 1% near the crest. Numerical evidence suggested that this occurs in a small boundary layer near the crest where $|\phi(s)|$ rises rapidly from $|\phi(0)| = 0$ and oscillates about $\pi/6$, the number of oscillations increasing as the maximum amplitude is approached.

McLeod derived, from Nekrasov's equation, the following integral equation

$$\phi(s) = \frac{1}{3\pi} \int_0^\infty \frac{\sin \phi(t)}{1 + \int_0^t \sin \phi(\tau) d\tau} \log \left| \frac{s-t}{s+t} \right| dt$$

for $\phi(s)$ in the boundary layer, whose width tends to zero as the maximum wave is approached. He also conjectured that the asymptotic form of $\phi(s)$ as $s \rightarrow \infty$ satisfies

$$\phi(s) = \frac{\pi}{6} \left\{ 1 + As^{-1} \sin(\beta \log s + c) + o(s^{-1}) \right\},$$

where A, β and c are constants with $\beta \approx 0.71$ satisfying the equation

$$\sqrt{3}\beta \tanh \frac{1}{2}\pi\beta = 1.$$

We solve McLeod's boundary layer equation numerically and verify the above asymptotic form.

1 Introduction

This paper considers the numerical solution of the equation

$$\phi(s) = \frac{1}{3\pi} \int_0^\infty \frac{\sin \phi(t)}{1 + \int_0^t \sin \phi(\tau) d\tau} \log \left| \frac{s+t}{s-t} \right| dt \quad (1.1a)$$

$$= -\frac{1}{3\pi} \int_0^\infty k(t, s) \{\psi(t) - \psi(s)\} dt, \quad (1.1b)$$

where

$$\psi(t) = \log \left(1 + \int_0^t \sin \phi(\tau) d\tau \right) \text{ and } k(t, s) = \frac{2s}{s^2 - t^2}. \quad (1.2)$$

This equation was derived by McLeod [1] to describe the boundary layer behavior of the solution, for large μ , near the origin of the equation

$$\phi_\mu(s) = \frac{1}{3\pi} \int_0^\pi \frac{\sin \phi_\mu(t)}{\mu^{-1} + \int_0^t \sin \phi_\mu(\tau) d\tau} \log \left| \frac{F(s+t)}{F(s-t)} \right| dt, \quad (1.3)$$

where $F(t) = \text{sn}(Kt/\pi)$ and sn denotes the Jacobian elliptic function with quarter periods K and iK' . Equation (1.3) was first formulated by Nekrasov [2] to describe waves of constant periodic form moving with constant speed on the surface of a non-viscous fluid that is either of infinite depth or on a horizontal bottom, when the flow is taken to be irrotational. The wave is assumed to be symmetric about its crest and the equation is derived by conformally mapping the region of the flow under one wavelength onto the unit disc cut along the negative real axis. The generic point on the circumference of the disc is e^{is} , with $-\pi < s < \pi$, and $s = 0$ corresponds to the crest. As the circumference is described in a clockwise direction from $-\pi$ to π the horizontal coordinate decreases by one wavelength. Then the function ϕ_μ is the angle that the wave surface makes with the horizontal. With this choice of coordinate $\phi_\mu(s)$ is periodic with period 2π . For more details, see Nekrasov [2],[3] and [4] or Milne-Thompson [5]. The wave is assumed to be symmetric about its crest. Thus $\phi_\mu(s)$ is an odd 2π periodic function of s with $\phi_\mu(0) = 0$. The solution is unique provided the additional assumption, that the wave has only one peak and one trough per period, is made. This is

$$\phi_\mu(s) > 0, \quad s \in (0, \pi) \text{ with } \phi_\mu(0) = \phi_\mu(\pi) = 0. \quad (1.4)$$

The constants K and iK' , the quarter periods of sn , are related to the depth h and wavelength, λ , by the relation

$$K'/K = h/\lambda. \quad (1.5)$$

As $h \rightarrow \infty$ we have $K \rightarrow \frac{1}{2}\pi$ ($K' \rightarrow \infty$) and $F(t) \rightarrow \sin \frac{1}{2}t$ so that (1.3) is also applicable for infinite depth. Equation (1.1) is derived by writing $\hat{s} = s\mu$ and writing $\phi_\mu(s\mu) = \hat{\phi}(\hat{s})$ and letting $\mu \rightarrow \infty$ with \hat{s} fixed. Then $\hat{\phi}(s)$ satisfies (1.1). The boundary layer behavior of the solution of (1.3) was established numerically by Chandler and Graham [6], who were able to obtain a solution with a maximum value of $\phi_\mu(s) \simeq 30 \cdot 3787 \dots^\circ$ and to detect a small number of oscillations about $\phi_\mu = 30^\circ$ for $\mu = 10^{18}$.

The numerical difficulty posed by the boundary layer behavior of the solutions of (1.3) for large μ is overcome, by Chandler and Graham [6], by using a non uniform mesh for the discretisation of (1.3). This consists of three regions: one to cope with the rapid variation of $\phi_\mu(s)$ in the boundary layer, whose thickness is of order μ^{-1} , near the origin; a second to deal with the slower variation away from the origin and a third for the transitional layer in between. For further references on the analytical properties of the solutions of (1.3) and related numerical results, see Chandler and Graham [6] and McLeod [1].

The purpose of this paper is to solve (1.1) numerically and show that the solution $\phi(s)$ oscillates about $\phi(s) = \pi/6$ and obeys the formal asymptotic result of McLeod [1] that can be written in the form

$$\phi(s) = \frac{\pi}{6} \left\{ 1 + \sum_{n=0}^{\infty} \frac{A_n}{s^n} \sin(n\beta \log s + c_n) \right\} \text{ as } s \rightarrow \infty, \quad (1.6)$$

where A_n and C_n are constants and $\beta = 0.71 \dots$ is the root of

$$\sqrt{3}\beta \tanh\left(\frac{1}{2}\pi\beta\right) = 1. \quad (1.7)$$

Equation (1.1) represents the solution in the boundary layer and can thus be solved with a uniform mesh size. However (1.1) has an additional complication compared with (1.3) in that the range of integration is infinite and the decay of the solution to its asymptotic limit is algebraic. This fact means that we require careful consideration in order to obtain an accurate numerical representation of the integral in (1.1).

2 The Numerical Method

Following Chandler and Graham [6] we solve the integral equation in the form (1.1b). This formulation is better, for numerical purposes, because the integration by parts that is used to convert (1.1a) to (1.1b), removes the logarithmic singularity, at $t = s$, which occurs in the kernel of (1.1a). Although the corresponding kernel of (1.1b) has a pole, the singularity of the integrand is removable since the multiple $\psi(t) - \psi(s)$, has a simple zero at $t = s$.

Thus we write

$$\phi(s) = \frac{1}{3\pi} \int_0^\infty K(t, s) dt, \quad (2.1)$$

where

$$K(t, s) = -\frac{2s(\psi(t) - \psi(s))}{s^2 - t^2} \quad t \neq s \quad (2.2a)$$

$$= \psi'(t) \equiv \frac{\sin \phi(t)}{1 + \int_0^t \sin \phi(\tau) d\tau} \quad t = s, \quad (2.2b)$$

the value in (2.2b) being the limit of the right hand side of (2.2a) as $|t - s| \rightarrow 0$.

We aim to set up a numerical approximation to the integral in terms of a discrete number of values $\phi(s_i)$, where $s_i = ih$, $0 \leq i \leq 2N$, with N an integer, for suitable choices of h and N and a continuous set of values $\phi(s)$ for $s \geq 2Nh$. Any values of $\phi(s)$ for $s < 0$ required by the numerical approximation are determined by the fact that $\phi(s)$ is an odd function of s . The numerical representation of the integral requires two approaches. The first is a finite difference formulation of the integral over a predetermined finite range using the discrete values of ϕ and the second is an estimation of the remainder using an appropriate asymptotic estimate of the values of $\phi(s)$ for $s \geq 2Nh$. The details of the asymptotic form of $\phi(s)$ as $s \rightarrow \infty$ that is used will be discussed later.

So we choose an appropriate end point $2T$ where T is given by $T = Nh$ and we can approximate the integral $I_1(s, \phi) = \int_0^{2T} K(t, s) dt$ using Simpson's Rule, since the integrand is analytic. The choice of the end point $2T$ is somewhat arbitrary. Eventually, see below, we will want to consider $I_1(s, \phi)$ for values of $s \leq T$. We choose an end point mT , with $m = 2$ in this case, so that the singularity of $k(t, s)$ at $t = s$ is far from the end point. The reason for this is that the remainder integral, again see below, requires a different evaluation and it is advantageous to make sure that the singularity of $k(s, t)$ is not close to the range of t in the remainder integral. This will become clearer when the evaluation of the remainder integral is discussed later.

Assuming that for large s , $\phi(s)$ is known in the form of an asymptotic expansion then truncation of this series, expansion of the integrand and a term by term integration of the integrand will give a suitable analytical estimate $EI_2(s, \phi)$ for the integral $I_2(s, \phi) = \int_{2T}^\infty K(t, s) dt$. Then we define the numer-

ical representation of the integral in (2.1) as

$$NI(s, \phi) = NI_1(s, \phi) + EI_2(s, \phi). \quad (2.3)$$

An alternative approach, assuming that the asymptotic form of $\phi(s)$, $s > T$, has been chosen, is to transform the infinite range of the remainder integral into a finite range, which can then be approximated numerically. For this purpose it is more convenient to revert to the integral in the form (1.1a) so we write

$$I_2(s) = \log\left(\frac{2T+s}{2T-s}\right) (\psi(2T) - \psi(s)) + \int_{2T}^{\infty} k_3(s, t) dt, \quad (2.4)$$

where

$$k_3(s) = \frac{\sin \phi(t)}{1 + \int_0^t \sin \phi(\tau) d\tau} \log\left(\frac{t+s}{t-s}\right) \quad (2.5)$$

If $\phi(t) \rightarrow \pi/6 + O(t^{-1})$ and $\int_0^\infty (\phi(t) - \pi/6) dt$ is bounded, it is easily established that $k_3(s, t) = 2st^{-2} + o(t^{-2})$ as $t \rightarrow \infty$. Thus the integral of k_3 , in (2.4) is convergent at infinity and the substitution $t = 2T/u$ transforms it to $\int_0^1 k_4(s, u) du$ with $k_4(s, 0) = s/T$. This integral can now be approximated using Simpson's rule with a suitably chosen step length. This approximation can be used instead of $EI_2(s, \phi)$ in (2.3).

Simpson's rule gives an approximation which is of order h^4 , but this rule requires an interval which consists of an even number of step lengths. However the integrand contains the function $\psi(t)$ which involves the determination of $\int_0^t \sin \phi(\tau) d\tau$ at values $t = t_i = ih$. To obtain a numerical approximation to this which is the same order as Simpson's rule for this integral we use an appropriate modified trapezoidal rule.

We now wish to solve the approximation

$$\phi(s) = \frac{1}{3\pi} NI(s, \phi). \quad (2.6)$$

To do this we define an approximation $\phi_N(s_i)$ to the solution $\phi(s)$ at the discrete values $s_i = ih$, $0 \leq i \leq N$. Using the same asymptotic form at the solution as that used to define $\phi(s)$ for $s \geq 2Nh$ we define the remaining discrete values of $\phi_N(s_i)$, $N+1 \leq i < 2Nh$, required for the evaluation of $NI_1(s)$ at the points $s = s_i$, $0 \leq i \leq N$.

Thus $\phi_N(s_i)$ satisfies the equations

$$\phi_N(s_i) = \frac{1}{3\pi} NI(s_i, \phi_N(s_j)), \quad 0 \leq i \leq N. \quad (2.7)$$

This gives, in a similar fashion to Chandler and Graham [6], a fully discrete non-linear system for the unknowns $\{\phi_N(s_i), i = 0..N\}$. This system is solved by the iterative method

$$\phi_N^m(s_i) = NI\left(s_i, \phi_N^{(m-1)}(s_j)\right), \quad i = 0..N, \quad (2.8)$$

starting from a suitable initial approximation $\phi_N^{(0)}(s_i)$. Chandler and Graham [6] were able to prove that, when the quadrature method used to approximate their integrals was the trapezoidal rule, convergence was guaranteed, although for computational purposes they opted for a more accurate scheme for computational purposes. Their proof cannot be extended to the numerical approximation used here even if the quadrature method is the trapezoidal rule because of the infinite range of integration. However we find that, as in the cases looked at by Chandler and Graham [6], the convergence rule is very quick.

3 The necessity of rescaling

We see from the definition of $K(t, s)$, (2.2a,b), and the fact that $\phi(0)$ is zero, that $NI(0, \phi) = 0$ provided the initial guess $\phi_N^{(0)}(0) = 0$. Then (2.7) gives $\phi_N^m(0) = 0$ for all $m > 0$. Thus effectively we can work with the N variables $\{\phi_N(s_i), i = 1..N\}$ and corresponding N equations from (2.7). One of the aims is to verify the asymptotic result (1.6). Initially we do not assume this and report here that for a variety of sensible choices of the asymptotic form of $\phi(s)$ we get rapid convergence to the solution of (2.8). Provided T is sufficiently large we can then numerically verify that (1.6) is the correct asymptotic result, using the computed values of $\phi(s)$ for $s \leq T$. Having verified this numerically to get the best accuracy we use (1.6) and find that as well as providing a more accurate numerical solution the convergence rate is also improved. The larger T is, the less necessary it is to have a large number of terms from (1.6) and in practice we use

$$\phi(s) = \frac{\pi}{6} \left(1 + \frac{A}{s} \sin(\beta \log s + c) \right), \quad s > T. \quad (3.1)$$

Table 1 shows the comparison of the location and the values of $\phi(s)$ at successive maximum and minimum values of ϕ and the comparison between this method at that of Chandler and Graham [6]. Before discussing this comparison we use the values of s at the successive turning points to illustrate the need for rescaling the variable s . It will become clear that the computations done to obtain table 1 could not be achieved by the method outlined in paragraph 1. We see that the s coordinate of each successive turning point increases by a factor of about 81, which is approximately the value of $e^{\pi/\beta}$. This is compatible with the set of turning points obtained from (3.1). The last turning point in $0 < s < T$ is located at $s = 2 \times 10^{11}$. Typically we used $h = 1/20$ as a sensible choice of h compatible with having a large enough T to capture the asymptotic behavior of the solutions. However with this choice of h it is not feasible to take $T = 2 \times 10^{11}$ as this would involve 4×10^{12} grid points. Typically using the scheme outlined in paragraph 1 we chose $T = 100$ and this does not even get to the first minimum of $\phi(s)$. However we learn from this initial attempt at a numerical solution that beyond $s = 100$, $6|\phi(s) - \pi/6|/\pi < 10^{-2}$ and varies very slowly. Thus for large s we do not need to take such a small step length.

For the numerical scheme we have used, we require a constant steplength so we make a simple change of independent variable. We wish to make no effective change at the origin but an exponential change at infinity so we use the transformation $s = e^y - 1$. Then with $t = e^z - 1$ and $\theta(y) = \phi(s(y))$, (1.1) becomes

$$\theta(y) = -\frac{1}{3\pi} \int_0^\infty \frac{2(e^y - 1)}{(e^y - e^z)(e^y + e^z - 2)} \log \left(\frac{1 + \int_0^z \sin \theta(\zeta)}{1 + \int_0^y \sin \theta(\zeta)} \right) dy, \quad (3.3)$$

We are then able to reduce the step length, h , and still take $T = e^{y_T} - 1$ to be large. Typically we take $h = 1/100$ and $y_T = 30$ giving $T = 1.0 \times 10^{13}$. This requires 3000 unknowns $\phi(y_i)$ where $y_i = ih$, $i = 1 \dots 3000$.

After the rescaling, the numerical scheme is essentially the same as that given in section 2 and is not repeated. However near $y = y_T$, $6|\theta(y) - \pi/6|/\pi$ is now of order 10^{-13} so the form of $\theta(y)$ effectively given by (3.1) will be accurate to 10^{-26} , that is $O(T^{-2})$.

4 The Numerical Results and Conclusions

All the numerical results given here are those produced by the numerical scheme outlined in Section 2 and 3 using the rescaled problem. Table 1 shows the comparison of the successive maxima and minima of $\phi(s)$ compared with those computed for the full problem by Chandler and Graham [6]. The position of these maxima and minima for the Chandler and Graham [6] computation, has been calculated by scaling their coordinate, s , by μ compatible with the boundary layer scaling used to derive (1.1) from (1.3). Thus $s = s_{B-S} = s_{CeG} \times \mu$. The number of decimal places given in table 1 for this numerical computation are as accurate as the numerical calculation will allow. There are three forms of error: the first comes from the order of the numerical approximation to the solution which is $O(h^4)$ which gives rise to errors of order 10^{-8} ; the second is due to machine accuracy which gives rise to an error of about 10^{-14} to 10^{-16} ; thirdly there is the error that arises when predicting the position and size of the maxima and minima of a function, from discrete data at given grid points, assuming that the data is accurate. The figures quoted in table 1 do not take into account the first of two of these sources of error.

The comparison with the computations of Chandler and Graham [6] is very good. The value at the first maximum is the same to eight significant figures and the position the same to six significant figures. The calculation of the value at the maximum always being more accurate than its positions. The values at the first minimum are in similar agreement although Chandler and Graham [6] only quote the position to four significant figures and the value at the minimum is only 4×10^{-3} below 30° so relatively the numbers do not appear to be in such good agreement as the value at the first maximum. The first noticeable divergence of the two computations appears at the second minimum where the estimates of the positions differ by about 4% although the values at this minimum are in good agreement given that they are both of order 10^{-7} below 30° . However the next maximum of Chandler and Graham [6] lies below 30° and it is apparent that at this value of s the effects of the outer solution, that is the decrease from the maximum on a slower scale, are just beginning to show. Presumably at this value of μ the oscillations in the Chandler and Graham [6] begin to cease at or around this value of s .

We wish to show that the solution behaves like (1.6) for large s . So for comparison we write $\Theta(x) = \phi(s)$, where $x = \frac{\beta}{\pi} \log s$ so that we expect

$$\Theta(x) \sim \frac{\pi}{6} \left\{ 1 + \frac{A}{s} \sin \pi(x - x_0) + \dots \right\} \text{ as } x \rightarrow +\infty \quad (4.1)$$

or

$$\Psi(x) \equiv \left(\frac{6}{\pi} \Theta(x) - 1 \right) s \sim A \sin \pi(x - x_0) + \dots, \quad (4.2)$$

Compared with the transformation (3.1) which has $y = 0$ when $s = 0$ we have $x \rightarrow -\infty$ as $s \rightarrow 0$. This makes $\left(\frac{6}{\pi} \Theta(x) - 1 \right) s \rightarrow 0$ as $x \rightarrow -\infty$ and introduces

a minimum of the function $\Psi(x)$ before the first maximum. The values of $x = x_i$ at the minima, maxima and the zeros of $\Psi(x)$ and the value of $\Psi(x)$ at the turning points are shown in table 2. If (4.2) were to be exact then the difference $x_i - x_{i-1} - 1/2 \equiv \Delta x_i$ would be zero and the magnitude of the value of $\Psi(x)$ at the turning points would be constant and equal to A . Included in this table are the computed values of Δx_i .

From the table we see that a good fit is obtained by choosing A and x_0 so that $\Psi(x)$ and (4.2) agree at the second maximum and fourth zero this gives

$$A = 1 \cdot 2364860386 \dots \text{ and } \tau_0 = 0 \cdot 72422 \dots \quad (4.3)$$

A plot of the asymptotic expression (4.2) with these values of A and x_0 and the comparison with $\Psi(x)$ is given in figure 1. The two graphs are indistinguishable from each other over a surprisingly large range of values of x , from before the first zero to beyond the sixth zero. The graphs start to diverge after this point. This is due to the fact that the exact solution of $\phi(s) - \pi/6$, or equivalently $\Psi(x)/s$, is so small in this range that round off error starts to become important and eventually dominates the solution. This is more apparent in figures 2 and 3 which plot the difference between $\Psi(x)$ and its asymptotic value. Figure 2 shows this difference multiplied by 100 in the range of values of x where the difference is less than one, while figure 3 shows 1000 times the difference. In both figures we see that the difference increases rapidly after $x \simeq 4$. It is particularly visible in figure 3 that this rapid rise has two different components: a systematic rise due to truncation error of the numerical scheme, which is of order 10^8 and a random error on the scale of about 10^{-14} , due to machine accuracy.

The last plot, figure 4, shows the difference between $\Psi(x)$ and its asymptotic value multiplied by s . This clearly shows that the dominant feature is one of a periodic function of period 1, compatible with a term proportional to $s^{-2} \sin 2\pi(x - x_1)$ that appears in (1.6).

To conclude we have presented a numerical scheme for the solution of (1.1), written in the form (3.3) which allows a sufficiently accurate numerical solution over a range $0 \leq s \leq 10^{13}$, that we can verify the predicted asymptotic form (1.6). The numerical calculation is limited by the two factors, truncation error and machine accuracy. The numerical solutions can be made more accurate by a higher order integration scheme but the range of integration is limited because the difference between the solution and $\pi/6$ becomes the same order of magnitude as the machine accuracy.

References

1. J.B. McLeod, The Stokes and Krasovskii Conjectures for the wave of greatest height. *Stud. App. Math.* 98: 311-333 (1997)
2. A.I. Nekrasov, *Izv. Ivanovo-Vosnosonk. Politehn Inst.* 3: 52-65 1921; 6:155-71 (1922)
3. A.I. Nekrasov, *Izv. Ivanovo-Vosnosonk. Politehn Inst.* 6:155-71 (1922)
4. A.I. Nekrasov, The exact theory of steady state waves on the surface of a heavy liquid. Technical Summary Report No 813. Mathematical Research center, University of Wisconsin, 1967 [D.V. Thampuran, translator:C.W. Cryer, editor]
5. L.M. Milne-Thompson, *Theoretical Hydrodynamics*, Macmillan, London, 1968.
6. G.A. Chandler and I.G. Graham, The Computation of water waves modelled by Nekrasov's Equation. *SIAM J. Numer. Anal.* 30: 1041-1065 (1993).

Figure Captions

Table 1. Positions of the turning points, s_t and the corresponding values, $\phi(s_t)$ and comparison with those obtained by Chandler and Graham.

Table 2. The positions, x_i of the zeros and the turning points of $s(\phi(s) - \pi/6)$ as a function of $x = \beta \log s$ and the corresponding values at the turning points. Δx_i is the difference $x_i - x_{i-1} - \frac{1}{2}$

Figure 1. Comparison $\Psi(x) \equiv (6\Theta(x)/\pi - 1)s$ with $A \sin(\pi(x - x_0))$ as a function of $x = \beta \log s/\pi$.

Figure 2. Difference between the solution and its Asymptotic form $100(\Psi(x) - A \sin(\pi(x - x_0)))$ as a function of $x = \beta \log s/\pi$.

Figure 3. Difference between the solution and its Asymptotic form $10000(\Psi(x) - A \sin(\pi(x - x_0)))$ as a function of $x = \beta \log s/\pi$.

Figure 4. Difference between the solution and its Asymptotic form $\Psi_1(x) \equiv s((6\Theta(x)/\pi - 1)s - A \sin(\pi(x - x_0)))$ as a function of $x = \beta \log s/\pi$.

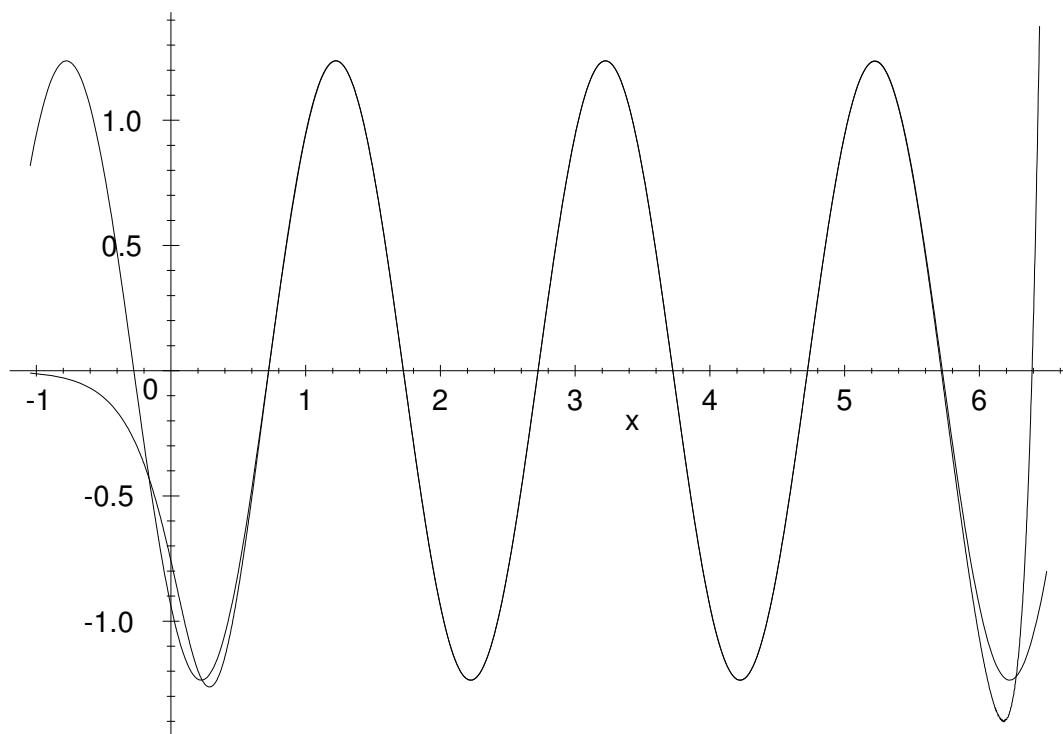


Figure 1. Comparison $\Psi(x) \equiv (6\Theta(x)/\pi - 1)s$ with $\text{Asin}(\pi(x - x_0))$ as a function of $x = \beta \log s / \pi$.

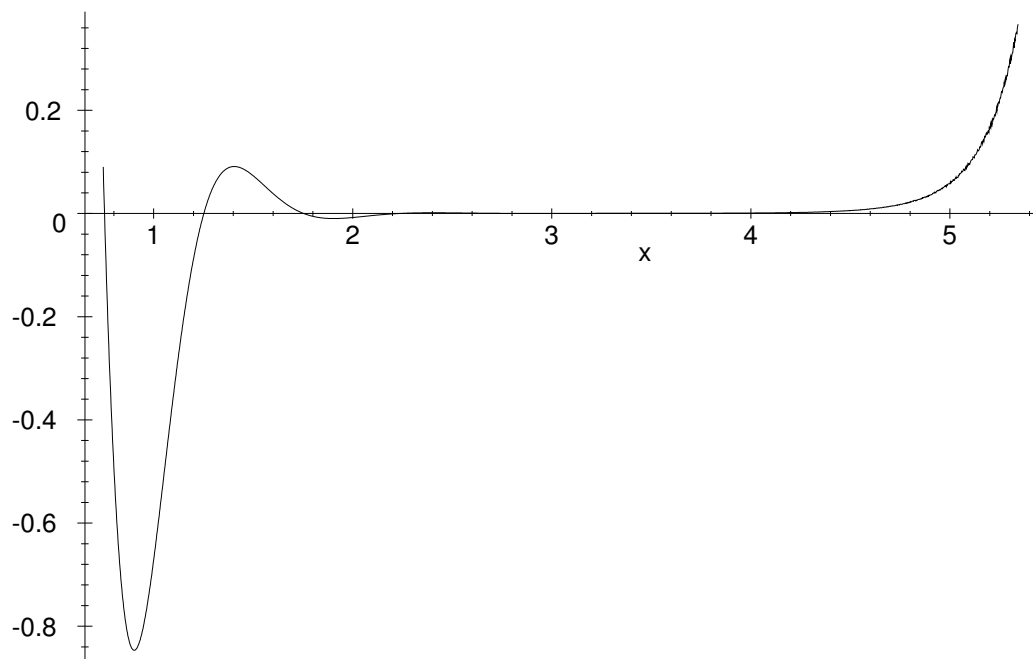


Figure 2. Difference between the solution and its Asymptotic form $100(\Psi(x) - A \sin(\pi(x - x_0)))$ as a function of $x = \beta \log s / \pi$.

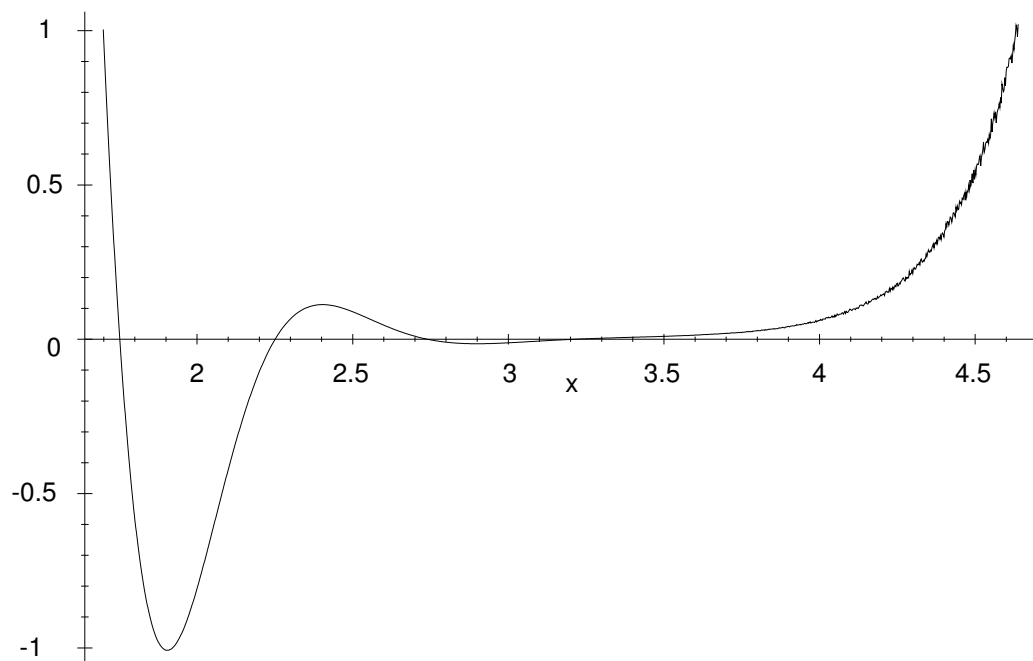


Figure 3. Difference between the solution and its Asymptotic form $10000(\Psi(x) - A \sin(\pi(x - x_0)))$ as a function of $x = \beta \log s / \pi$.

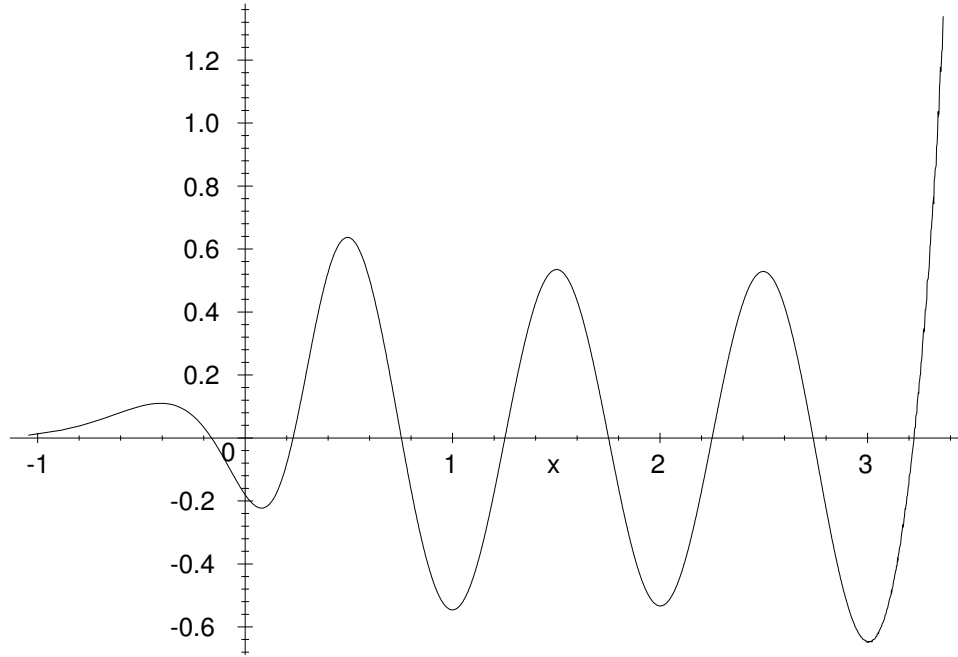


Figure 4. Difference between the solution and its Asymptotic form
 $\Psi_1(x) \equiv s((6\Theta(x)/\pi - 1)s - A \sin(\pi(x - x_0)))$ as a function of $x = \beta \log s/\pi$.

TABLE 1: Positions of the turning points, s_t and the corresponding values, $\phi(s_t)$ and comparison with those obtained by Chandler and Graham.

s_t This paper	s_t C. & G.	$6\phi(s_t)/\pi - 1$	$\phi(s_t)^o - 30^o$	$\phi(s_t)^o - 30^o$ C. & G.
5.706256×10^1	5.7062493×10^1	$1.26234416 \times 10^{-2}$	$3.787032480 \times 10^{-1}$	$3.787032466 \times 10^{-1}$
4.683476245×10^3	4.683×10^3	$-1.5345108772 \times 10^{-4}$	$-4.6035326316 \times 10^{-3}$	-4.60353×10^{-3}
$3.80716.261 \times 10^5$	3.807×10^5	$1.88776874 \times 10^{-6}$	$5.66330622 \times 10^{-5}$	5.6631×10^{-5}
3.09513×10^7	3.21×10^7	-2.322037×10^{-8}	-6.966111×10^{-7}	-7.4218×10^{-7}
2.51266×10^9	2.416×10^8	2.8545×10^{-2}	8.5635×10^{-9}	-3.6722×10^{-7}
2.058×10^{11}		-3.96×10^{-12}	-1.188×10^{-10}	

TABLE 2: The positions, x_i of the zeros and the turning points of $s(\phi(s) - \pi/6)$ as a function of $x = \beta \log s$ and the corresponding values at the turning points. Δx_i is the difference $x_i - x_{i-1} - \frac{1}{2}$

Nature of point	x_i	Δx_i	$s(6\phi(s)/\pi - 1)$
1 st . Minimum	0.285868285199		-1.263432342282
1 st . Zero	0.72529360368	-.06057468	
1 st . Maximum	1.22279723767	-.00249637	1.236931699148
2 nd . Zero	1.724207968438	.00141073	
2 nd . Minimum	2.224237124	.00002916	-1.23648103488
3 rd . Zero	2.7242200786	-.00001705	
2 nd . Maximum	3.224219455	-.00000062	1.23648608360
4 th . Zero	3.724219486	.00000003	
3 rd . Minimum	4.2242314	.00001191	-1.23650251
5 th . Zero	4.72425830	.00002690	
3 rd . Maximum	5.222	-.00225830	1.234586
6 th . Zero	5.716482352	-.00551765	